Accepted Manuscript

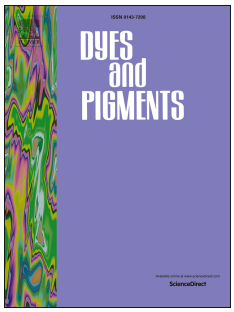

A highly selective naked-eye and fluorescent probe for fluoride ion based on 1,8-naphalimide and benzothizazole

Xiaoxing Chen, Taohua Leng, Chengyun Wang, Yongjia Shen, Weihong Zhu

PII: S0143-7208(16)31410-3

DOI: 10.1016/j.dyepig.2017.02.008

Reference: DYPI 5785

To appear in: *Dyes and Pigments*

Received Date: 14 December 2016

Revised Date: 6 February 2017

Accepted Date: 7 February 2017

Please cite this article as: Chen X, Leng T, Wang C, Shen Y, Zhu W, A highly selective naked-eye and fluorescent probe for fluoride ion based on 1,8-naphalimide and benzothizazole, *Dyes and Pigments* (2017), doi: 10.1016/j.dyepig.2017.02.008.

Graphical Abstract

A highly selective naked-eye and fluorescent probe for fluoride ion based on 1,8-naphalimide and benzothizazole

Xiaoxing Chen, Taohua Leng, Chengyun Wang , Yongjia Shen, and Weihong Zhu

A novel near-infrared fluorescent probe with high sensitivity and selectivity for fluoride ion has been fabricated.

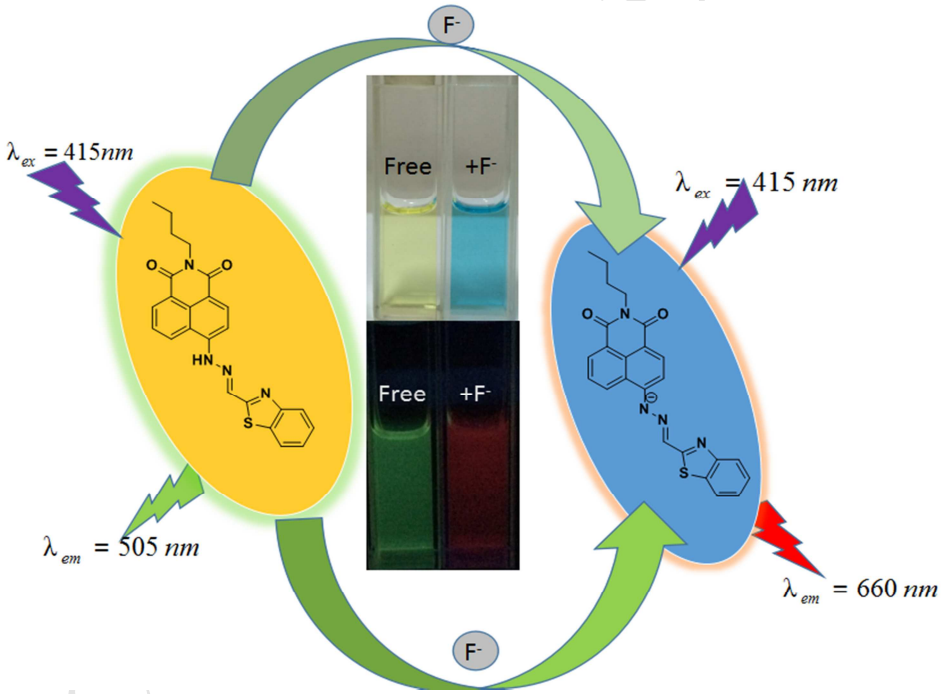

A highly selective naked-eye and fluorescent probe for fluoride ion based on 1,8-naphalimide and benzothizazole

Xiaoxing Chen [a], Taohua Leng [b], Chengyun Wang [a,] *, Yongjia Shen[a], and Weihong Zhu [a,]*

[a] *Shanghai Key Laboratory of Functional Materials Chemistry, Key Laboratory for Advanced Materials and Institute of Fine Chemicals, School of Chemistry and Molecular Engineering, East China University of Science and Technology, 130 Meilong Road, Shanghai 200237, China*

[b] *National Food Quality Supervision and Inspection Center (Shanghai) / Shanghai Institute of Quality Inspection and Technical Research, Shanghai 200233, China.*

Abstract

Based on benzothizazole and 1,8-naphalimide, a novel colorimetric and fluorescent probe (probe **1**) for fluoride ion was synthesized by Schiff base reaction. The striking yellow-to-blue color change of the probe **1** in the CH_3CN was observed with the naked eyes only in presence of F^- among the eight anions (F^-, Cl^-, Br^-, I^-, NO_3^-, HSO_4^-, $H_2PO_4^-$, AcO^-). Besides that, upon addition of F^-, both of the absorption and emission peaks shifted to near-infrared region (NIR) (>600 nm) in UV-vis and fluorescent spectra, and the detection limit reached as low as 0.41μM. Furthermore, the ^1H NMR titration and theoretical calculation based on TD-DFT indicated that the fluoride ion induced deprotonation of the probe **1** through hydrogen bonding interaction between

* Corresponding author. Tel./fax: +86-021-64252967; e-mail: cywang@ecust.edu.cn; whzhu@ecust.edu.cn

amino group of probe **1** and fluoride ion.

Key words

Fluoride ion; fluorescent probe; 1, 8-napthalimide; benzothizazole

1. Introduction

In recent years, the design of methods to selectively recognize and detect various anions has emerged as a research area of great importance [1-4] due to the major roles of the anions in chemical, biological and environmental assays [5-7]. Among the various anions, fluoride ion, with the smallest ionic radius, highest charge density and a hard Lewis basic nature [8-10], is closely associated with human health. For example, excessive intake of fluoride could induce many diseases such as fluorosis, urolithiasis, acute gastric, kidney problems and even cancer [11]. In addition, fluoride has also been applied in military areas such as nuclear weapon manufacture [2] and nerve gas monitor [12, 13]. As a result, convenient and efficient detection techniques for fluoride ion have attracted great attention and many achievements have been reported [14-20]. Compared with the traditional detection techniques including electrode method and ^{19}F-NMR analysis [21], colorimetric and fluorescent probe methods have drawn increasing attention from scientists who are devoted to studying host/guest and supramolecular chemistry because of their operational simplicity, high sensitivity, low detection limit and bioimaging analysis in vivo, even in living cells [22-25]. Up to date, some probes for fluoride ion have been developed, most of which are mainly based on molecular interactions between the receptor and fluoride [26],

such as hydrogen bonding [26-32], B-F complexation [1, 33-35] and desilylation of Si-O/Si-C bonds [36-39].

Among them, probes for fluoride ion based on hydrogen bond generally utilize the N-H of urea, sulfonamide, pyrrole, indole and amide. However, probes used the hydrazone as hydrogen bond donor are rare. In some case, these receptors may also respond to other anions like $H_2PO_4^-$ and AcO^- or only show colorimetric responses to fluoride ion. Thus, it is extremely necessary to develop the colorimetric and fluorescent probe with high selectivity.

In this paper, a new hydrazone receptor (probe **1**) containing 1,8-naphthalimide and benzothiazole was designed and synthesized through Schiff base reaction (Scheme 1). As one of the classical fluorophore, 1,8-naphthalimide has been widely used by various receptors due to its many excellent properties, such as good photostability, high fluorescence quantum yields, large Stokes' shift. In addition, benzothiazole was chosen to append to the –NH-N= moiety for two main reasons: (i) the presence of the benzothiazole as electron-withdrawing substituent group is expected to enhance the acidity and propitious to deprotonation of probe **1** as consequence; (ii) The benzothiazole unit can broaden conjugation structure of the system after deprotonation of probe **1**. According to the ICT mechanism, probe **1** maybe show peaks red-shifts and intensity changes in UV-vis and fluorescent spectra [2], therefore it can be used as probe for F^-. Actually, Probe **1** showed high selectivity for fluoride ion through the deprotonation action, and it could detect fluoride ion by ratiometric colorimetric and fluorescent methods which was observable with the naked eyes

within 10 s, the detection limit reached as low as 0.41μM.

Insert **Scheme 1** here

2. Experimental section

All the starting materials, reagents and solvents were AR grade and purchased from J&K chemical Co., which were received without further purification. ^{1}H and ^{13}C NMR spectra were measured on a Bruker AM-400 spectrometer at room temperature using d-chloroform or DMSO-d_6 as a solvent and tetramethylsilane (TMS, δ= 0 ppm) as an internal standard. The UV-vis spectra were recorded on a Nicolet CARY 100 and the fluorescence spectra were measured on a CARY Eclipse. The stock solutions of probe **1** (1.0×10^{-5}mol/L) were prepared in DMSO solution. The TBA salts (F^-, Cl^-, B^-, I^-, NO_3^-, HSO_4^-, $H_2PO_4^-$, AcO^-) solutions were prepared at a concentration of 0.01 mol/L in CH_3CN solution. Different equivalents of TAB salts were added to the probe **1** and their corresponding UV-vis and fluorescence spectra were recorded at room temperature. Probe **1** (1.0×10^{-5}mol/L in CH_3CN) was titrated with fluoride anion (as tetrabutylammonium salts) by addition of increasing equivalents of anion in DMSO-d_6 solution. The energies and oscillator strengths with 80-120 lowest energy electronic transitions were obtained using time-dependent DFT (TD-DFT) with Becker's three parameterized Lee-Yang-Par(B3LYP) exchange functional with 6-31G(d) and 6-31G**+Lanl2DZ basis sets.

2.1 Synthesis of *4-bromo-N-butyl-1,8-naphthalimide* (compound **2**)

The mixture of 4-bromo-1,8-naphthalic anhydride (5.000 g, 18.000 mmol) (70 mL)

and 1-aminobutane (1.700 g, 23.400 mmol) in ethanol was refluxed for 6 h under nitrogen atmosphere. The mixture was then cooled to the room temperature and filtered. The filter cake was washed three times with ethanol and the crude product was recrystallized from ethanol to obtained a pale yellow solid [40] (5.220 g, 87%).^{1}H NMR (400 MHz, DMSO-d_6, TMS): δ_H 8.54-8.49 (m, 2H)， 8.30 (d, *J*=7.6 Hz, 1H), 8.19 (d, *J*=7.6 Hz, 1H), 7.97 (t, *J*=7.2 Hz, 1H), 4.02 (t, *J*=7.2 Hz, 2H), 1.61 (m, 2H), 1.41-1.31 (m, 2H), 0.93 (t, *J*=7.6 Hz, 3H). ^{13}C NMR (100 MHz, DMSO-d_6) δ_C 162.639, 162.588, 132.377, 131.374, 131.172, 130.750, 129.545, 128.986, 128.592, 127.993, 122.491, 121.712, 29.492, 19.776, 13.665.

2.2 Synthesis of *4-hydrazine hydrate-N-butyl-1,8-naphthalimide* (compound **3**)

4-Bromo-N-butyl-1,8-naphthalimide (3.300 g, 10.000 mmol) and 2.5 mL hydrazine hydrate (85%, w/w) were added into 50 mL ethylene glycol monomethyl ether and the mixture was refluxed for 6 h. After cooled to the room temperature, the mixture was poured into 80 mL water and the precipitated solid was filtered, dried in vacuum to give a red solid [14] (2.250 g, 80%).^{1}H NMR (400 MHz, DMSO-d_6, TMS): δ_H 9.12 (s, 1H), 8.61 (d, *J*= 8.4 Hz, 1H), 8.41 (d, *J*= 7.2 Hz, 1H), 8.28 (d, *J*= 8.8 Hz, 1H), 7.63 (t, *J*=7.6 Hz, 1H), 7.24 (d, *J*=7 Hz, 1H), 4.67 (s, 2H), 4.01 (t, *J*=7.2Hz, 2H), 1.58 (m, 2H), 1.33 (m, 2H), 0.92 (t, *J*= 7.2 Hz, 3H). ^{13}C NMR (100 MHz, DMSO-d_6) δ_C 163.695, 162.843, 153.108, 134.108, 130.461, 129.213, 128.142, 124.008, 121.668, 118.346, 107.330, 103.910, 29.805, 19.826, 13.717.

2.3 Synthesis of *benzo[d]thiazol-2-ylmethanol* (compound **4**)

To mixture of 2-aminobenzenethiol (25.000 g, 0.200 mol) and glycolic acid (46.000 g, 0.600 mol) was added HCl (4 N, 60 mL). The reaction was allowed to proceed under reflux at 100 °C for 6 h prior to being quenched with saturated aqueous sodium bicarbonate. The solution was extracted three times with ethyl acetate. The combined extracts were evaporated in vacuum to give the crude product. The crude product was purified by chromatography on a silica gel column with DCM/MeOH (100/2, v/v) as the eluent to yield compound **4** [41] (3.630 g, 11%). ^{1}H NMR (400 MHz, $CDCl_3$, TMS): δ_H 7.97 (d, *J*=8.0 Hz, 1H), 7.88 (d, *J*=7.6 Hz, 1H), 7.47 (t, *J*=7.2 Hz, 1H), 7.38 (t, *J*=7.2 Hz, 1H), 5.75 (br, 1H), 5.08 (s, 2H). ^{13}C NMR (100 MHz, $CDCl_3$) δ_C 173.635, 152.634, 134.528, 126.218, 125.099, 122.569, 121.841, 62.237.

2.4 Synthesis of *Benzothiazole-2-carbaldehyde* (compound **5**)

To a solution of benzothiazol-2-ylmethanol (1.650 g, 10.000 mmol) in methylene chloride (40mL) was added DMP (4.600 g, 31.000 mmol), and the reaction was allowed to proceed with stirring at 4 °C for 1 h prior to being quenched with saturated aqueous sodium thiosulfate solution. The subsequent mixture was extracted three times with methylene chloride. The combined organic extracts were dried with anhydrous magnesium sulfate and concentrated. The crude product was purified by chromatography on a silica gel column, eluting with DCM/MeOH (100/1, v/v) to yield the product benzothiazole-2-carbaldehyde [41] (0.650 g ,40%). ^{1}H NMR (400 MHz, $CDCl_3$, TMS): δ_H 10.18 (s,1H), 8.25 (d, *J*=7.6 Hz, 1H), 8.02 (d, *J*=7.6 Hz, 1H), 7.61 (m, 2H). ^{13}C NMR (100 MHz, $CDCl_3$) δ_C 184.432, 164.377, 135.263, 127.359, 126.966, 124.728, 121.649.

2.5 Synthesis of probe **1**

A mixture of benzothiazole-2-carbaldehyde (1.630 g, 1.000 mmol), 4-hydrazinehydrate-N-butyl-1,8-naphthalimide (0.283g, 1.000 mmol) and a drop of acetic acid was heated to reflux for 4 h in 10 ml ethanol. After cooling to the room temperature, many precipitates were formed. The precipitates were collected through filtration and recrystallized from ethanol to give pale yellow probe **1** (0.359 g, 84%). MP: 194.5-195.5 °C. ^{1}H NMR (400 MHz, DMSO-d_6, TMS): δ_H 12.05 (s, 1H), 8.78 (d, *J*=8.4 Hz, 1H), 8.68 (s, 1H), 8.52 (d, *J*=7.2 Hz, 1H), 8.02 (d, *J*=8.0 Hz, 1H), 7.87 (t, *J*=8.4 Hz, 1H), 7.73 (d, *J*=8.4 Hz, 1H), 7.57-7.47 (m, 2H), 4.03 (t, *J*=7.2 Hz, 2H), 1.61 (m, 2H), 1.35 (m, 2H), 0.93 (t, *J*=7.2 Hz, 3H). IR (KBr: v (cm^{-1})): 3445, 3222, 2960, 1682, 1647, 1587, 1566, 1387, 1242, 1120, 1020. HRMS (EI): m/z Calcd for $C_{24}H_{20}N_4O_2S_1$ $[M]^-$, 428.1307; found, 428.1308. Anal. Calcd for $C_{24}H_{20}N_4O_2S_1$: C, 67.27; H, 4.70; N, 13.07%. Found: C, 67.23; H, 4.66; N, 13.11%.

3. Results and discussion

3.1 Colorimetric analysis

The interactions of probe **1** with various anions (F^-, Cl^-, Br^-, I^-, NO_3^-, HSO_4^-, $H_2PO_4^-$, AcO^-) were firstly investigated in CH_3CN through colorimetric analysis. These anions mentioned were prepared in TBA salts form. Upon addition of 5 equiv of fluoride anion, the solution color of probe **1** (1.0×10^{-5}mol/L in CH_3CN) changed from yellow to blue under ambient light and fluorescence color of probe 1 changed from green to red under a UV lamp at 365 nm, yet no appreciable color changes were observed when 5 equiv of other anions (Cl^-, Br^-, I^-, NO_3^-, HSO_4^-, $H_2PO_4^-$, AcO^-) were added

(Fig.1). Thus, the detection of probe **1** for F^- can be observed through naked eyes.

Insert **Fig. 1** here

3.2 UV-vis and fluorescence emission studies in CH_3CN

The interactions between probe **1** and various anions (F^-, Cl^-, Br^-, I^-, NO_3^-, HSO_4^-, $H_2PO_4^-$, AcO^-) were studied by UV-vis absorption and fluorescence titration. The titrations were carried out in CH_3CN by addition of 0.01 mol/L corresponding anions (F^-, Cl^-, Br^-, I^-, NO_3^-, HSO_4^-, $H_2PO_4^-$, AcO^-) to solution of probe **1** (1.0×10^{-5} mol/L). As shown in Fig 2a, probe **1** possessed a certainly strong absorption band centered at 445 nm. Upon the addition of F^-, the intensity of absorbance at 445 nm decreased gradually while a new peak at 620 nm appeared and developed. And then, the band reached the maxima at 5 equiv of F^-. Meanwhile, five clear isosbestic points were observed at 248 nm, 280 nm, 334 nm, 381 nm and 494 nm, indicating that only one product was generated during the titration process. Besides, the fluorescence titrations (Fig.2b) demonstrated that probe **1** exhibited emission at 505 nm when it was excited at 410 nm. When F^- was added to the solution of probe **1**, a drastic decrease of emission at 505 nm and the emergence of a red-shifted emission band centered at 660 nm in near-infrared (NIR) region, were observed with a clear iso-emission point at 629 nm. These UV-vis and fluorescence spectral changes could be attributed to the hydrogen-bond interaction between F^- with the amino proton of probe **1** and the following deprotonation of amino group [2] (Scheme 2). Analogous UV-vis and

fluorescence experiments were also carried out with other anions (Cl^-, Br^-, I^-, NO_3^-, HSO_4^-, $H_2PO_4^-$, AcO^-) (Fig. 3a, Fig. 3b and blue bars of Fig. S1). Upon addition of 50 equiv of these anions, only AcO^- showed dinky interference while other anions have no interference in the detection of F^- with UV-vis and fluorescence spectroscopy methods. To further assess its utility as an F^- selective probe, its UV-vis spectra response to F^- in presence of other anions was also tested. The test results were the same as the results mentioned above (white bars of Fig. S1). These results strongly indicated that probe **1** can detect F^- as a colorimetric and fluorescent probe with high selectivity.

Insert **Fig. 2** here

Insert **Scheme 2** here

Insert **Fig. 3** here

3.3 Determination of the stoichiometric ratio and association constant

Continuous variation methods were applied to determine the stoichiometric ratio of probe 1 with fluoride ion. A Job-plot (Fig. 4a) of probe **1** with fluoride ion in CH_3CN showed the maxima at 0.5 of $[F^-]$ / ($[F^-]$ + [probe **1**]). The phenomenon indicated that the probe 1 associated with fluoride ion in 1:1 ratio during the initial stage of the reaction. The binding stoichiometry of probe **1** with fluoride ion also calculated by the Benesi-Hildebrand equation:

A_0 is the absorbance of free probe **1**, A_∞ is the absorbance treated with excess amount of F^-, A is the absorbance treated with a certain concentration of fluoride ion, K is the

binding constant (M^{-1}) and $[F^-]_0$ is the concentration of fluoride ion (M). The plot of 1/ ($A-A_0$) against 1/ $[F^-]_0$ showed linear relationship (R=0.994) (Fig. 4b), indicating that probe **1** bound to fluoride ion in 1:1 stoichiometry. The association constant K between probe **1** and fluoride ion was determined from the ratio of intercept/slope to be 1.46×10^4 M^{-1}.

Insert **Fig. 4** here

3.4 Detection mechanism

The proposed binding mechanism of probe **1** with F^- is shown in Scheme 2. To interpret F^- sensing mechanism of probe **1**, ^1H NMR titration experiments were carried out in DMSO-d_6. Fig. 5 showed partial ^1H NMR spectrum of interaction of probe **1** and F^-. The signal of NH proton decreased and became broader after the addition of 0.05 equiv F^-, implying that fluoride ion could complex with probe **1** because of the hydrogen–bond interactions existed between amino proton of probe **1** and fluoride at low concentration of TBAF. On the further addition of more than 2 equiv of F^-, the resonance signal of the N-H proton disappeared. Meanwhile the chemical shift values of aromatic protons occurred to slightly changes. These results suggested that the amino group of probe **1** would be deprotonated when the F^- concentration turned higher.

Insert **Fig. 5** here

To further interpret the interaction between the F^- and probe **1**, theoretical calculations based on time-dependent density functional theory (TD-DFT) were carried out. As

shown in Table 1 and Table 2, the highest occupied molecular orbitals (HOMO) of probe 1 and $1+F^-$ were located at the conjugated units of probe **1**, and the lowest unoccupied molecular orbitals (LUMO) of the probe **1** and $1+F^-$ were mainly located at the 1,8-naphthalimide unit. The strongest absorption at 445 nm of probe 1 contributed to the charge transfer transition from benzothiazole to 1, 8-naphthalimide. After adding fluoride ion, the charge of product $1+F^-$ transferred from the amino group to the 1,8-naphthalimide unit, which could be used to explain the new absorption at 620 nm. In addition, Fig. S2 and Table S1 (See in ESI) clearly showed that the calculated UV-vis spectra of probe **1** and $1+F^-$ were in agreement with the experimental results, implying that the sensing mechanism that we proposed is reasonable.

Insert **Table 1** here

Insert Table 2 here

4. Conclusion

In summary, a ratiometric colorimetric and fluorescent receptor (probe **1**) for fluoride ion was designed and synthesized via Schiff base reaction. Probe **1** shows good selectivity, high sensitivity, and fast response to fluoride ion. Moreover, it presents dramatic color change, which can be observed directly by naked eyes and displays optical response in near-infrared (NIR) region (>600 nm) after addition of fluoride ion in 10 s. We believe these characteristics of probe **1** are very important and promising in the sensing fluoride ion.

Acknowledgments

The authors are grateful to financial support from the National Natural Science Foundation of China (No. 21576087) and Natural Science Foundation of Shanghai (16ZR1408000).

References

[1] Zhou Y, Zhang JF, Yoon J. Fluorescence and colorimetric chemosensors for fluoride ion detection. Chem Rev 2014;114(10):5511-71.

[2] Liu B, Tian H. A ratiometric fluorescent chemosensor for fluoride ions based on a proton transfer signaling mechanism. J Mater Chem 2005;15(27 -28):2681.

[3] Kim HN, Guo Z, Zhu W, Yoon J, Tian H. Recent progress on polymer-based fluorescent and colorimetric chemosensors. Chem Soc Rev 2011;40(1):79-93.

[4] Lee M, Jo S, Lee D, Xu Z, Yoon J. A new naphthalimide derivative as a selective fluorescent and colorimetric sensor for fluoride, cyanide and CO_2. Dyes Pigments 2015;210: 288-292.

[5] Shang XF, Xu XF. The anion recognition properties of hydrazone derivatives containing anthracene. Bio Systems 2009;96(2):165-71.

[6] Xu Z, Tang J, Tian H. A highly sensitive colorimetric and ratiometric sensor for fluoride ion. Chin Chem Lett 2008;19(11):1353-7.

[7] Saravana Kumar M, Ashok Kumar SL, Sreekanth A. Highly selective fluorogenic anion chemosensors: naked-eye detection of F^- and AcO^- ions in natural water using a test strip. Anal Methods 2013;5(22):6401.

[8] Zhang JF, Zhou Y, Yoon J, Kim JS. Recent progress in fluorescent and colorimetric chemosensors for detection of precious metal ions (silver, gold and platinum ions). Chem Soc Rev 2011;40(7):3416-29.

[9] Cao XW, Lin WY, Yu QX, Wang JJ. Ratiometric sensing of fluoride anions based on a BODIPY-Coumarin Platform. Org Lett 2011:13(22):6089-6101.

[10] Guo ZQ, Song NR, Moon JH, Yoon J, et al. A benzobisimidazolium-based fluorescent and colorimetric chemosensor for CO_2. J. Am. Chem. Soc. 2012, 134: 17846−17849

[11] Fu L, Wang F-F, Gao T, Huang R, He H, Jiang F-L, et al. Highly efficient fluorescent BODIPY dyes for reaction-based sensing of fluoride ions. Sens Actuators B 2015;216:558-62.

[12] Sohn H, Létant S, Sailor M J, et al. Detection of fluorophosphonate chemical warfare agents by catalytic hydrolysis with a porous silicon interferometer. J Am Chem Soc 2000, 122(22): 5399-5400.

[13] Zhang S W, Swager T M. Fluorescent detection of chemical warfare agents: Functional group specific ratiometric chemosensors. J Am Chem Soc 2003, 125(12): 3420-3421.

[14] Liu C, Xu J, Yang F, Zhou W, Li Z, Wei L, et al. Nanomolar Cu^{2+} and F^{-} naked-eye detection with a 1,8-naphthalimide-based colorimetric probe. Sens Actuators B 2015;212:364-70.

[15] Gai L, Chen H, Zou B, Lu H, Lai G, Li Z, et al. Ratiometric fluorescence chemodosimeters for fluoride anion based on pyrene excimer/monomer

transformation. Chem Commun 2012;48(87):10721-3.

[16] Ke IS, Myahkostupov M, Castellano FN, Gabbai FP. Stibonium ions for the fluorescence turn-on sensing of F^- in drinking water at parts per million concentrations. J Am Chem Soc 2012;134(37):15309-11.

[17] Liu XM, Zhao Q, Song WC, Bu XH. New highly selective colorimetric and ratiometric anion receptor for detecting fluoride ions. Chem Eur J 2012;18(10):2806-11

[18] Xiong L, Feng J, Hu R, Wang S, Li S, Li Y, et al. Sensing in 15 s for aqueous fluoride anion by water-insoluble fluorescent probe incorporating hydrogel. Anal Chem. 2013;85(8):4113-9.

[19] Yang Y, Zhao Q, Feng W, Li F. Luminescent chemodosimeters for bioimaging. Chem Rev 2013;113(1):192-270.

[20] Hou P, Chen S, Wang H, Wang J, Voitchovsky K, Song X. An aqueous red emitting fluorescent fluoride sensing probe exhibiting a large Stokes shift and its application in cell imaging. Chem Commun 2014;50(3):320-2.

[21] Konieczka P, Zygmunt B, Namiesnik J. Comparison of Fluoride Ion-Selective Electrode Based Potentiometric Methods of Fluoride Determination in Human Urine. Bull Environ Contam Toxicol 2000;64(6):794-803.

[22] Ke IS, Myahkostupov M, Castellano FN, Gabbai FP. Stibonium ions for the fluorescence turn on sensing of F^- in drinking water at parts per million concentrations. J Am Chem Soc 2012;134(37):15309-11.

[23] Xiong L, Feng J, Hu R, Wang S, Li S, Li Y, et al. Sensing in 15 s for aqueous

fluoride anion by water-insoluble fluorescent probe incorporating hydrogel. Anal Chem 2013;85(8):4113-9.

[24] Yang Y, Zhao Q, Feng W, Li F. Luminescent chemodosimeters for bioimaging. Chem Rev 2013;113(1):192-270.

[25] Hou P, Chen S, Wang H, Wang J, Voitchovsky K, Song X. An aqueous red emitting fluorescent fluoride sensing probe exhibiting a large Stokes shift and its application in cell imaging. Chem Commun 2014;50(3):320-2.

[26] Zheng X, Zhu W, Liu D, Ai H, Huang Y, Lu Z. selective colorimetric/fluorometric dual-channel fluoride ion probe, and its capability of differentiating cancer cells. ACS Appl Mater Interfaces. 2014;6(11):7996-8000.

[27] Xu Z, Kim SK, Yoon J. Revisit to imidazolium receptors for the recognition of anions: highlighted research during 2006-2009. Chem Soc Rev 2010;39(5):1457-66.

[28] Guo Z, Shin I, Yoon J. Recognition and sensing of various species using boronic acid derivatives. Chem Commun 2012;48(48):5956-67

[29] Tan W, Zhang D, Wang Z, Liu C, Zhu D. 4-(N, N-Dimethylamine)benzonitrile (DMABN) derivatives with boronic acid and boronate groups: new fluorescent sensors for saccharides and fluoride ion. J Mater Chem. 2007;17(19):1964.

[30] Li Q, Guo Y, Xu J, Shao S. Novel indole based colorimetric and "turn on" fluorescent sensors for biologically important fluoride anion sensing. J Photochem Photobiol B 2011;103(2):140-4.

[31] Yu M, Xu J, Peng C, Li Z, Liu C, Wei L. A novel colorimetric and fluorescent

probe for detecting fluoride anions: from water and toothpaste samples. Tetrahedron. 2016;72(2):273-8.

[32] Diao Q, Ma P, Lv L, Li T, Sun Y, Wang X, et al. A water-soluble and reversible fluorescent probe for Al^{3+} and F^{-} in living cells. Sens Actuators B 2016;229:138-44.

[33] Wang Y, Zhao Q, Zang L, Liang C, Jiang S. Discriminating detection of multiple analytes (F^{-} and CN^{-}) by a single probe through colorimetric and fluorescent dual channels. Dyes Pigments 2015;123:166-75.

[34] Du W, Xu J, Li H, Feng C, Yu M, Li Z, et al. Naked-eye and fluorescence detection of basic pH and $F^{-}$with a 1,8-naphthalimide-based multifunctional probe. RSC Adv 2015;5(20):15077-83.

[35] Wu J, Lai G, Li Z, Lu Y, Leng T, Shen Y, et al. Novel 2,1,3-benzothiadiazole derivatives used as selective fluorescent and colorimetric sensors for fluoride ion. Dyes Pigments 2016;124:268-76.

[36] Zhu B, Yuan F, Li R, Li Y, Wei Q, Ma Z, et al. A highly selective colorimetric and ratiometric fluorescent chemodosimeter for imaging fluoride ions in living cells. Chem Commun 2011;47(25):7098-100.

[37] Zhang J F, Lim C S, Bhuniya S, et al. A highly selective colorimetric and ratiometric two-photon fluorescent probe for fluoride ion detection. Org Lett 2011, 13(5): 1190-1193.

[38] Xu J, Sun S, Li Q, Yue Y, Li Y, Shao S. A novel "Turn-On" fluorescent probe for F^{-} detection in aqueous solution and its application in live-cell imaging. Anal

Chim Acta. 2014;849:36-42.

[39] Xu X, Chen Y, Wei L, Mao W, Lin F, Zhou X. Fluorescent turn-on probes for the detection of fluoride ions in organic solvent and in cells. Anal Methods 2016;8(2):245-8.

[40] Zhang W, Huo F, Liu T, Wen Y, Yin C. A rapid and highly sensitive fluorescent imaging materials for thiophenols. Dyes Pigments 2016;133:248-54.

[41] Wang R, Chen C, Zhang X, Zhang C, Zhong Q, Chen G, et al. Structure-Activity Relationship and Pharmacokinetic Studies of 1,5-Diheterorylp-enta-1,4-dien-3-ones: A Class of Promising Curcumin-Based Anticancer Agents. J Med Chem 2015;58(11):4713-26.

Scheme captions:

Scheme 1 Synthetic route of probe **1**

Scheme 2 Proposed sensing mechanism toward F^-

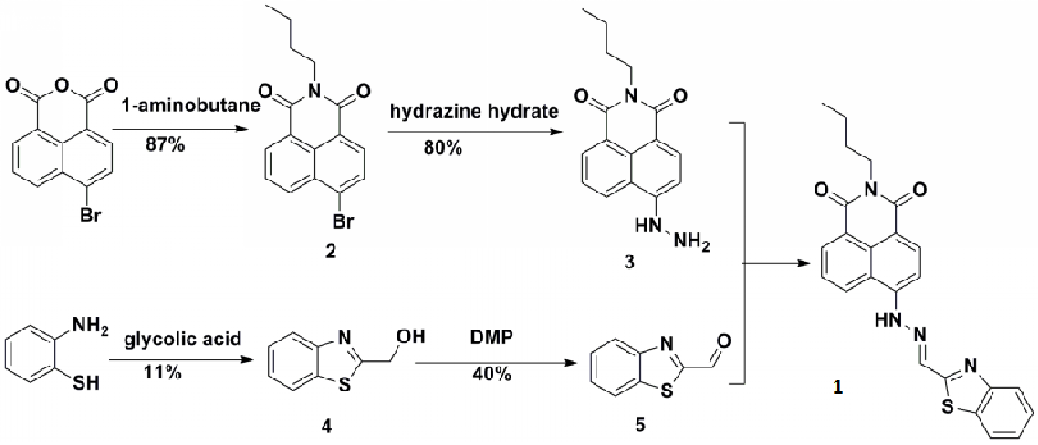

Scheme 1 Synthetic route of probe **1**

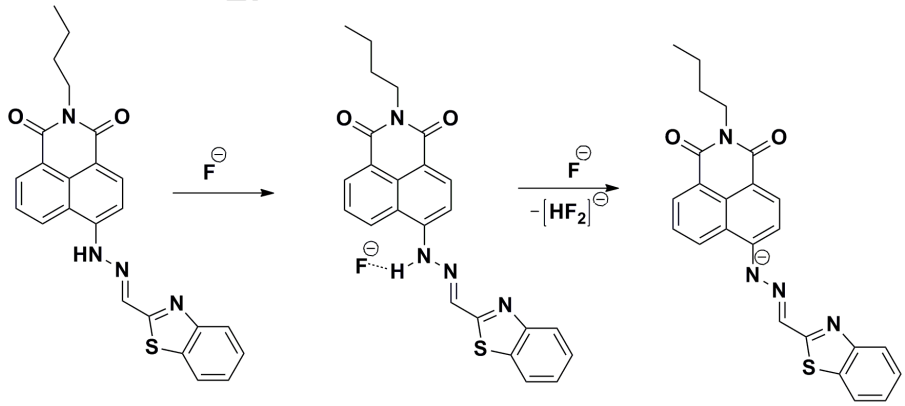

Scheme 2 Proposed sensing mechanism toward F^-

Table captions:

Table 1. Computed energy levels of frontier molecular orbitals

Table 2. Calculated surfaces of HOMO-1, HOMO, LUMO, and LUMO+1 of probe **1** and **1**+F^-

Table 1

Computed energy levels of frontier molecular orbitals

	HOMO-1(eV)	HOMO(eV)	LOMO(eV)	LUMO+1(eV)	HOMO-LUMO(eV)
Probe 1	**-6.56**	**-5.66**	**-2.54**	**-1.85**	**3.12**
1+F$^-$	**-5.79**	**-4.51**	**-2.02**	**-1.09**	**2.49**

Table 2

Calculated surfaces of HOMO-1, HOMO, LUMO, and LUMO+1 of probe **1** and **1+F$^-$**

	HOMO-1	HOMO	LUMO	LUMO+1
Probe 1	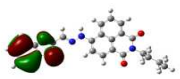	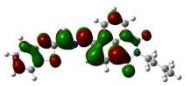		
1+F$^-$	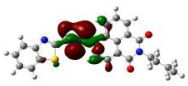	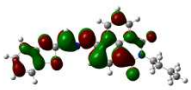		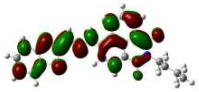

Figure captions:

Fig. 1 Color changes of probe **1** (1.0×10^{-5} mol/L in CH_3CN) with the addition of 5 equiv of various anions (0.01 mol/L in CH_3CN) (Cl^-, Br^-, I^-, F^-, NO_3^-, HSO_4^-, $H_2PO_4^-$, AcO^-) under ambient light (top) and a UV lamp at 365 nm (bottom)

Fig. 2 (a) UV-vis absorption and **(b)** emission spectra of probe **1** (1.0×10^{-5}mol/L in CH_3CN) in presence of TBAF (0.01mol/L in CH_3CN)

Fig. 3 (a) UV-vis absorption and **(b)** emission spectra of probe **1** (1.0×10^{-5}mol/L in CH_3CN) in the present of 50 equiv of other anions (Cl^-, Br^-, I^-, NO_3^-, HSO_4^-, $H_2PO_4^-$, AcO^-) (0.01mol/L in CH_3CN) and 5 equiv of F^- (0.01mol/L in CH_3CN).

Fig. 4 (a) Job's plot for complexation of probe 1 (620nm) with F^- determined by UV-vis absorbance in CH_3CN ($[F^-]$ + [probe **1**]) = 1.0×10^{-5}mol/L at 298 K. **(b)** Benesi-Hildebrand plot of UV-vis titration results probe **1** (1.0×10^{-5}mol/L) at 445 nm with F^- (0.01 mol/L).

Fig. 5. ^1H NMR titration spectra of probe **1** in DMSO-d_6 in presence of various equivalents of TBAF.

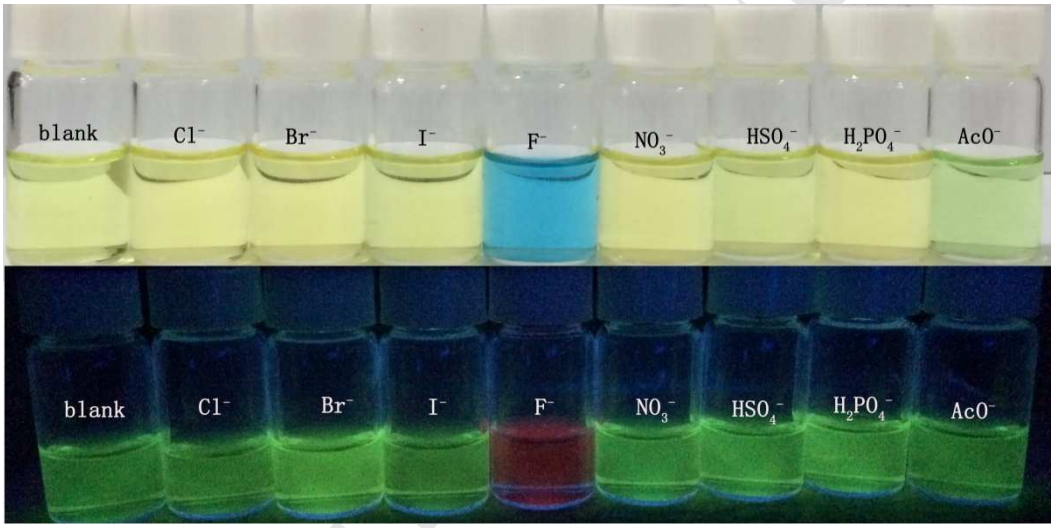

Fig. 1 Color changes of probe **1** (1.0×10^{-5} mol/L in CH_3CN) with the addition of 5 equiv of various anions (0.01 mol/L in CH_3CN) (Cl^-, Br^-, I^-, F^-, NO_3^-, HSO_4^-, $H_2PO_4^-$, AcO^-) under ambient light (top) and a UV lamp at 365 nm (bottom)

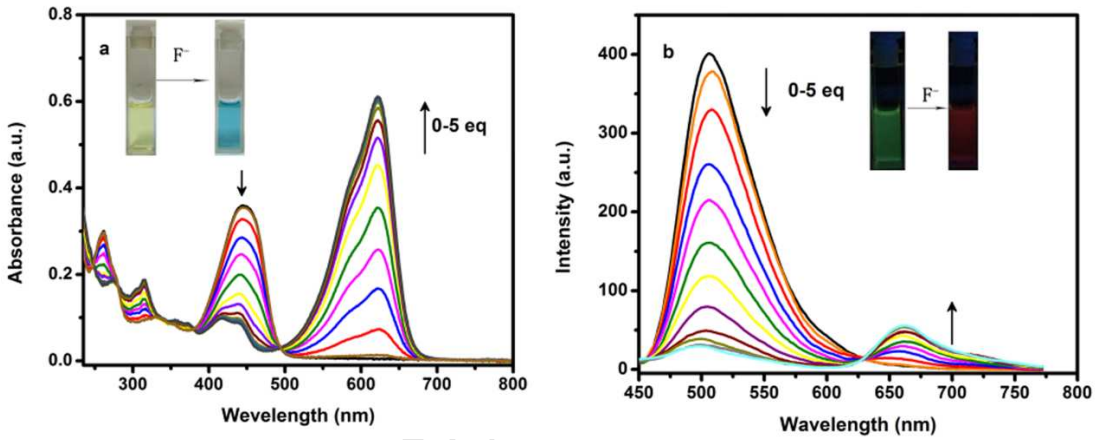

Fig. 2 (a) UV-vis absorption and **(b)** emission spectra of probe **1** (1.0×10^{-5}mol/L in CH_3CN) in presence of TBAF (0.01mol/L in CH_3CN)

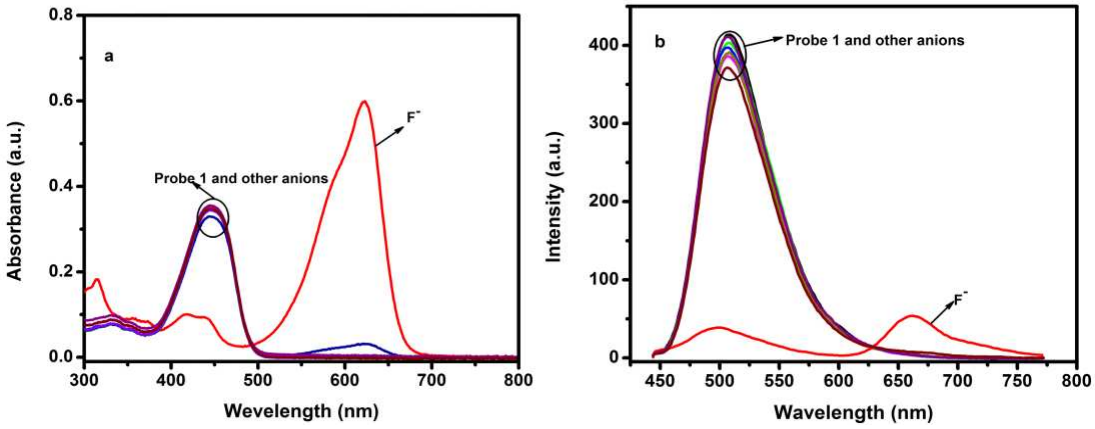

Fig. 3 (a) UV-vis absorption and **(b)** emission spectra of probe **1** (1.0×10^{-5}mol/L in

CH_3CN) in the present of 50 equiv of other anions (Cl^-, Br^-, I^-, NO_3^-, HSO_4^-, $H_2PO_4^-$, AcO^-) (0.01mol/L in CH_3CN) and 5 equiv of F^- (0.01mol/L in CH_3CN).

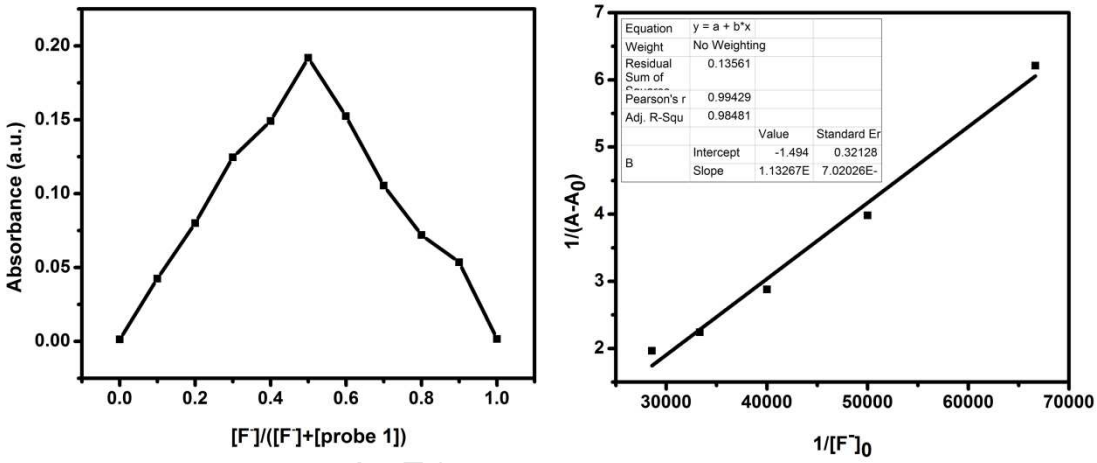

Fig. 4 (a) Job's plot for complexation of probe **1** (620nm) with F^- determined by UV-vis absorbance in CH_3CN ($[F^-]$ + [probe **1**]) = 1.0×10^{-5}mol/L at 298 K. **(b)** Benesi-Hildebrand plot of UV-vis titration results probe **1** (1.0×10^{-5}mol/L) at 445 nm with F^- (0.01 mol/L).

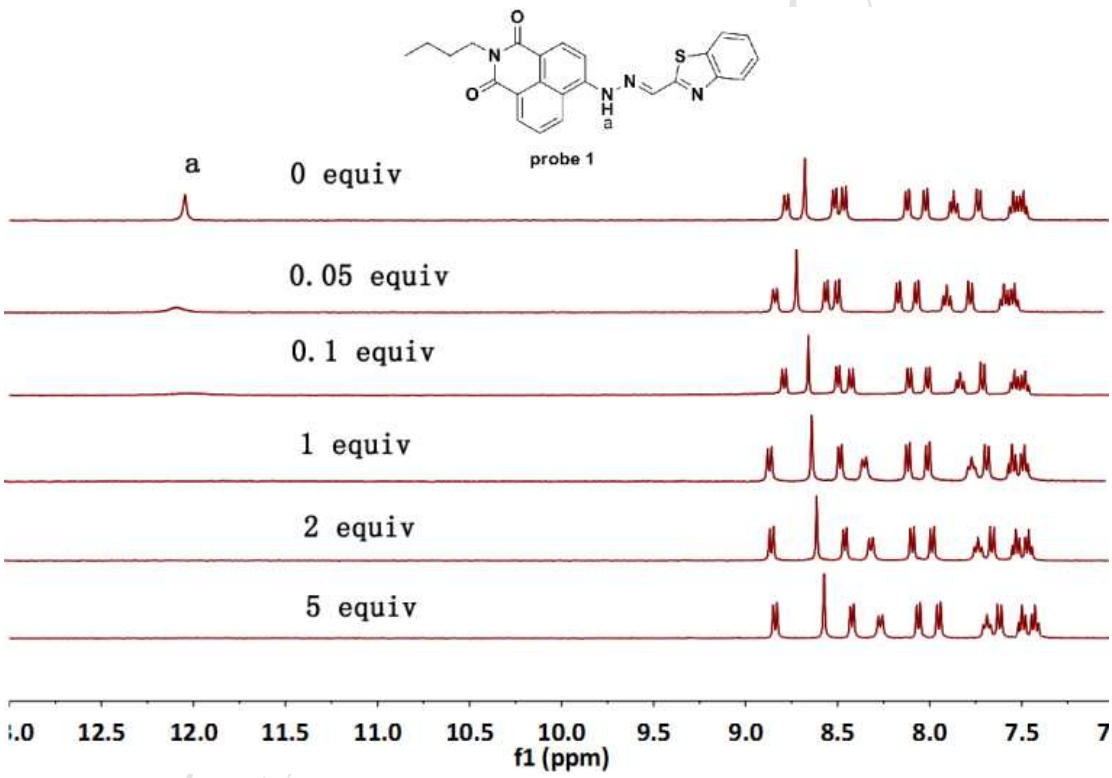

Fig. 5. ^{1}H NMR titration spectra of probe **1** in DMSO-d_6 in presence of various equivalents of TBAF.

Highlights

- The obvious color and fluorescence changes can be observed with naked eyes.
- Probe **1** possesses good selectivity, low detection limit and fast response for F^-.
- Probe **1** displays ratiometric optical response to F^- in near-infrared (NIR) region